UNIVERSITY OF PARDUBICE

FACULTY OF CHEMICAL TECHNOLOGY

Department of General and Inorganic Chemistry

Ondřej Mrózek

Impact of intramolecular coordination on the hapticity of indenyl ligand

Theses of the Doctoral Dissertation

Pardubice 2019

Study program: **Inorganic Chemistry**

Study field: **Inorganic Chemistry**

Author: Ing. **Ondřej Mrózek**

Supervisor: **prof. Ing. Jaromír Vinklárek, Dr.**

Year of the defense: 2019

Reference

MRÓZEK, Ondřej. *Impact of intramolecular coordination on the hapticity of indenyl ligand*. 2019. Dissertation thesis (Ph.D.). University of Pardubice, Faculty of Chemical Technology, Department of General and Inorganic Chemistry. Supervisor prof. Ing. Jaromír Vinklárek, Dr.

Abstract

This doctoral thesis is combined experimental/theoretical study focused on the indenyl complexes of molybdenum and tungsten, which contain intramolecular coordination. Among studied possible donor-acceptor interaction (e.g., S → Mo, N → W), the N → M coordination from the 1-(quino-8-yl)indenyl ligand was found to stabilized η^2-propene complexes, allowing their isolation and full characterization. To our best knowledge, the crystal structure of this type of alkene complexes was obtained for the very first time, providing unambiguous proof that the η^2-propene compounds are formed within allyl protonation using a strong acid for complexes of the type $[(\eta^5\text{-Cp}')(\eta^3\text{-allyl})M(CO)_2]$. Subsequently, it was found that particular monodentate ligands (CH_3CN) might exchange η^2-bonded alkene and induce haptotropic rearrangement. The obtained low hapticity complexes show a stable η^3-coordination of the indenyl with no tendency to reverse ring slippage in coordinating or non-coordinating solvents. This phenomenon was further studied in terms of quantum-chemical calculation, which revealed the nature of stabilized η^3-indenyl coordination using intramolecular coordination. The crucial outcome of this theoretical study is that the activation energy of haptotropic rearrangement is considerably dependent on the rotation of the indenyl. In the case of complexes with strong intramolecular coordination, the intrinsic hemilability of indenyl is forbidden due to the blocked indenyl rotation. This phenomenon seems to be a general aspect of transition metal indenyl complexes and should be kept in mind within a design of new catalysts.

Abstract

Tato disertační práce je zaměřena na kombinované experimentální/teoretické studium indenylových komplexů molybdenu a wolframu, které obsahují intramolekulární koordinaci. Prostřednictvím N → M (M= Mo, W) interakce z 1-(chino-8-yl)indenylového ligandu bylo možné připravit, isolovat a plně charakterizovat stabilizované η^2-propenové komplexy. Vůbec poprvé byla u tohoto typu alkenových sloučenin získána krystalová struktura, která jednoznačně potvrdila vznik η^2-propenových komplexů při protonaci allylového ligandu pomocí silné kyseliny u komplexů typu $[(\eta^5\text{-Cp}')(\eta^3\text{-allyl})M(CO)_2]$. Následně byla studována reaktivita těchto sloučenin a bylo zjištěno že určité monodentátní ligandy (CH_3CN) mohou substituovat propen a zároveň indukovat $\eta^5 \rightarrow \eta^3$ haptotropní přesmyk. U získaných sloučenin s nízkou hapticitou indenylu byla, pomocí multinukleární NMR spektroskopie, popsána neobvykle stabilní η^3-koordinace, která nevykazuje tendenci ke zpětnému $\eta^3 \rightarrow \eta^5$ přesmyku v koordinujícím ani nekoordinujícím rozpouštědle. Tento fenomén byl dále studován pomocí kvantově-chemických výpočtů, které objasnily podstatu stabilizace

nízkého koordinačního módu π-ligandu prostřednictvím intramolekulární koordinace. Klíčovým výstupem je zjištění, že rotace indenylového ligandu zásadně ovlivňuje aktivační energii haptotropního přesmyku. Tedy silná, ireverzibilní intramolekulární interakce může blokovat hemilabilitu indenylu, v důsledku zabránění rotace, což se zdá být obecný fenomén, který by měl být zohledněn při návrhu katalyzátorů na bázi Ind ligandu.

Keywords

haptotropic rearrangement, molybdenum, tungsten, intramolecular coordination, propene

Klíčová slova

haptotropní přesmyk, molybden, wolfram, intramolekulární koordinace, propen

Table of Contents

Introduction

Indenyl (Ind), which might be considered as a benzannulated derivative of cyclopentadienyl (Cp) is widely used spectator ligand in organic synthesis and catalysis.[1] The main advantage of Ind comparing to the Cp ligand, is generally low activation energy of haptotropic rearrangement. This so-called "Indenyl effect" allows prompt switch of the π-ligand to lower coordination mode meaning intrinsic hemilability of Ind, which is indeed a desirable aspect of potential catalysts. To rationalize the design and development of indenyl-base catalyst, the detailed knowledge of mechanisms of haptotropic rearrangements and possible routes how to influence it (e.g. induce or block) is necessary. The sixth group metal Ind species are very suitable for the study of the haptotropic rearrangements since the dynamic behavior was reported at room temperature for complexes with unsubstituted indenyl ligand: $[(\eta^3\text{-Ind})Mo(NCCH_3)_3(CO)_2][BF_4] \leftrightarrow [(\eta^5\text{-Ind})Mo(NCCH_3)_5(CO)_2][BF_4]$.[2] In this case, the coordination sphere of the complex or indenyl ligand itself might be easily adjust, and subsequently, the impact of these modifications on the haptotropic shift could be evaluate at room temperature. In fact, certain studies, using this system, have been already reported. For example, the introduction of a tridentate ligand into the coordination sphere leads to the stabilization of low-hapticity mode. For this type of stabilization were used 1,4,7-trimethyl-1,4,7-triazacyclononane, various tris(pyrazolyl) borates or cyclic polythioethers.[2–5] The coordination of these type of ligands leads to the exchange of the acetonitriles, and the strong chelate effect does not allow the reverse haptotropic shift back to η^5 mode. Another approach of the stabilization of low-hapticity complexes uses bulky *N*,*N*-chelating ligands, e.g., 2,9-dimethyl-phenanthroline.[6] In this case, sterically demanding chelate leads to preferable η^3-coordination of the indenyl, which minimalizes steric repulsion.

Although the haptotropic rearrangement of the indenyl ligand raises considerable attention during last two decades, the impact of strong intramolecular coordination on the hapticity of Ind has not been revealed yet, which is the primary goal of this doctoral thesis.

1. State-of-Art

1.1 Indenyl complexes with intramolecular coordination

In numerous of indenyl-based catalytically active species, an intramolecular interaction from the π-ligand moiety is a part of the structure. This motif, described e.g. for Cr^{III} indenyl complexes, provides additional stabilization effect to give highly active catalysts, stable at room temperature.[7] However, in certain cases, the significant decreases of the reactivity were observed due to the incorporation of the strong intramolecular interaction to a coordination sphere of a complex. This effect was demonstrated on titanium compounds of type [(η^5:η^1-IndCH_2CH_2NR)$TiMe_2$], where R is aryl or alkyl substituent.[8] In this case, the side chain of the indenyl ligand is connected with the central atom *via* covalent amido-bond. These complexes were tested as a catalyst for hydroamination of alkynes revealing rather average activity, which was attributed to the irreversible intramolecular coordination that might affect haptotropic rearrangement of the pi-ligand.[8]

1.2 Indenyl molybdenum compounds

In the middle of nineties, Romão et al. studied the reactivity of indenyl molybdenum complex [(η^5-Ind)Mo$(NCCH_3)_2(CO)_2$][BF_4].[2,9] The weakly bonded acetonitrile ligands might be easily exchanged using various monodentate (e.g., DMF, PMe_3) or bidentate ligands (e.g., 2,2'-bipyridine, ethylenediamine).[9–11] Moreover, in the presence of an excess of acetonitrile, the $\eta^5 \leftrightarrow \eta^3$ haptotropic rearrangements were observed. This process was comprehensively studied using NMR spectroscopy, including VT-NMR experiment, and the dynamic process [(η^5-Ind)Mo$(NCCH_3)_2(CO)_2$][BF_4] ↔ [(η^3-Ind)Mo$(NCCH_3)_3(CO)_2$][BF_4], which undergoes at room temperature was unambiguously proved (**Scheme 1**).

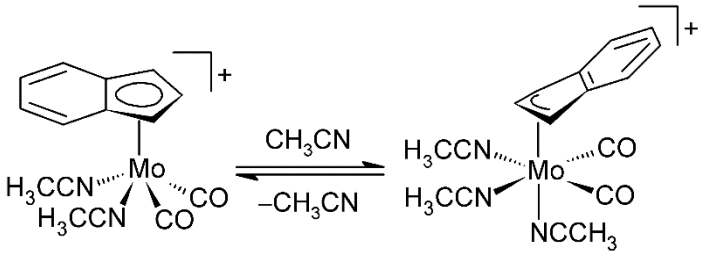

Scheme 1 Haptotropic rearrangement of indenyl molybdenum complexes.

The hapticity of indenyl ligand might be easily determined using ^1H and ^{13}C spectroscopy. In the case of η^5-indenyl, the signals of *ipso*-carbons (C^{3a} and C^{7a}) and protons H^2 are located in the relatively high field (~110 and ~5.5 ppm respectively). For the η^3-indenyl these signals are considerably shifted to lower field (up to ~150 and ~7.0 ppm respectively). This pattern was found for the aforementioned system in the spectra measured at –40ºC, which suggested that the activation barrier of haptotropic rearrangement could not be overcome at low temperature.

2 Goals of the thesis

As described above, the intramolecular interaction from the indenyl side chain, which is a relevant strategy for the stabilization of catalysts, might affect the reactivity of the resulting complexes considerably. Since this phenomenon might be connected with ring slippage of the Ind moiety, the primary target of this thesis is to describe the impact of intramolecular coordination on the hapticity of indenyl ligand. To fulfil the primary goal, the following partial steps may be formulated:

(a) synthesis organometallic compounds of Mo and W, with indenyl ligand substituted by various donor atoms,

(b) synthesis of the complexes with intramolecular coordination,

(c) evaluate the impact of intramolecular coordination on haptotropic shift using experimental techniques and theoretical calculations.

Ad (a) in this work, several derivatives of indenes were designed. The first one, 1-($C_4H_3SCH_2$)C_9H_7 (**1**), contain thiophene fragment in the side chain. The sulfur atom of this heterocycle contains two lone pairs, suitable for the formation of desired intramolecular coordination. The indenes 1-($C_9H_6NCH_2$)C_9H_7 (**2**) and 3-(C_9H_6N)C_9H_7 (**3**) are based on the highly basic aromatic amines. **Ad** (b) next step is focused on the synthesis of starting complexes of the type [(η^3-allyl)(η^5-Ind')$M(CO)_2$], where Ind' is derivative of indenyl based on the pro-ligands **1**–**3**. The key reaction of these compounds is protonation of the allyl ligand, where the formation of cation species with desired intramolecular coordination is expected. **Ad** (c) in the case of the complexes with intramolecular interaction the reactivity with various monodentate ligands, that might induce haptotropic shift (mainly CH_3CN), will be studied. The ring slippage in solution might be easily monitored using ^{13}C and ^{1}H NMR spectroscopy. Moreover, for the synthesized system, the theoretical calculation will be used for the evaluation of energy profiles of the haptotropic shifts.

3 Methods

All operations were performed under an argon atmosphere by using conventional Schlenk-line techniques. Infrared spectra were recorded in the 4000–400 cm^{-1} region with a Nicolet iS50 FTIR spectrometer using a diamond smart orbit ATR. ^{1}H and $^{13}C\{^{1}H\}$ APT, ^{19}F and ^{11}B NMR spectra were measured at 300 K on a Bruker 400 Avance and a Bruker 500 Avance spectrometer. The ^{1}H and ^{13}C resonances were assigned using 2D techniques including ^{1}H-^{1}H COSY, ^{1}H-^{13}C HSQC or ^{1}H-^{13}C HMBC. The chemical shifts are given in ppm relatively to residual signals of the solvent [^{1}H, ^{13}C: C_6D_6 (7.16, 128.39 ppm); CD_2Cl_2 (5.32, 54.00 ppm), CD_3CN (1.94, 118.69 ppm)] or external standard [^{11}B: $B(OMe)_3$, 18.10 ppm; ^{19}F: $CFCl_3$, 0.00 ppm]. Crystallographic data were collected either on Nonius KappaCCD diffractometer equipped with Bruker APEX-II CCD detector by monochromatized MoKα radiation (λ = 0.71073 Å) or on Bruker D8 VENTURE Kappa Duo PHOTON100 by IμS micro-focus sealed tube MoKα radiation (λ = 0.71073 Å).

All calculations were performed with the Gaussian 09[12] software package by using the B3LYP exchange–correlation functional[13–16] in combination with the cc-pVDZ-PP basis set.[17] The geometry optimizations were performed without symmetry constrains. Transition-state optimizations were performed with synchronous transit-guided quasi-Newton method (STQN).[18,19] Frequency calculations were performed to confirm the nature of the minima and stationary points. One imaginary frequency was observed for each transition state and none for the minima. Each transition state was further confirmed by following the intrinsic reaction coordinate (IRC) on both sides. The solvent effects were considered in all energy calculations by using polarizable continuum model (PCM). [20]

4 Results and Discussion

4.1 Synthesis of substituted indenes

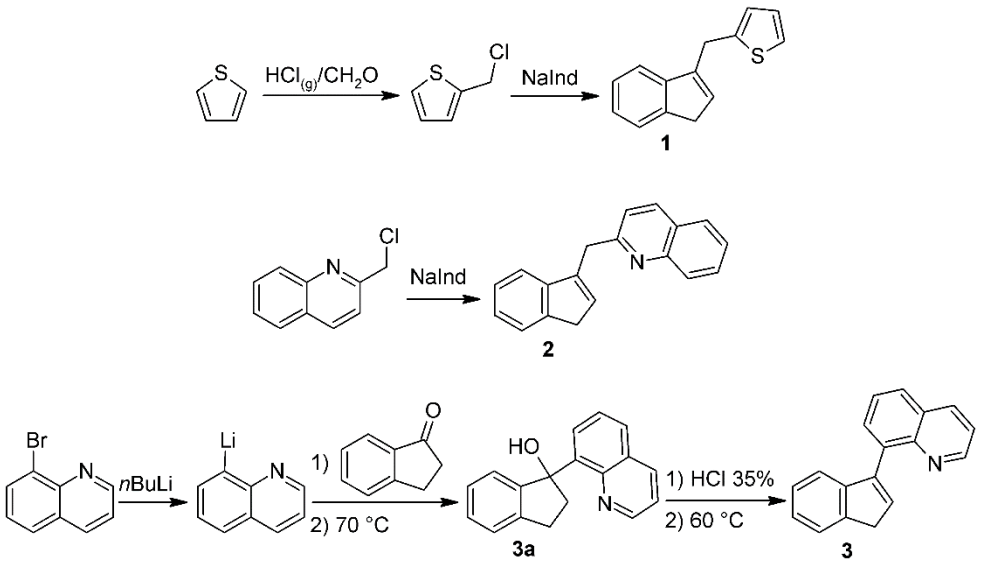

Scheme 2 Synthesis of substituted indenes **1**–**3**.

Indenes 1-($C_4H_3SCH_2$)C_9H_7 (**1**) a 1-($C_9H_6NCH_2$)C_9H_7 (**2**) were prepared using the reaction of (chloromethyl) derivatives of corresponding heterocycles with sodium indenide (**Scheme 2**). The 2-(chloromethyl)thiophene was prepared by using the protocol described in the literature using the one-pot reaction of hydrogen chloride, formaldehyde and thiophene.[21] This synthetic approach gives a mixture of mono- and di-substituted thiophenes easily separable by vacuum distillation. The 2-(chloromethyl)quinoline is available commercially as the hydrochloride. The quinolyl substituted indene 3-(C_9H_6N)C_9H_7 (**3**) is readily accessible by the well-known reaction of the 8-lithioquinoline with 1-indanone following by acid-catalyzed dehydration.[22]

4.2 Synthesis and characterization of allyl complexes

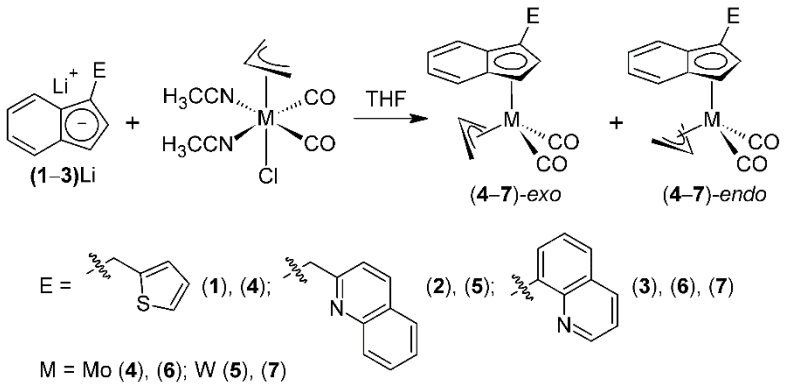

Scheme 3 Synthesis of allyl/indenyl complexes **4**–**7**.

The indenes **1**–**3** were firstly lithiated with *n*BuLi and then mixed with starting complex [(η^3-C_3H_5)$M(CO)_2(NCMe)_2Cl$], where M = Mo, W. After work-up the allyl-indenyl complexes [(η^3-C_3H_5)(η^5-Ind')$M(CO)_2$], where M = Mo, Ind' =

1-($C_4H_3SCH_2$)C_9H_6 (**4**); M = W, Ind' = 1-($C_9H_6NCH_2$)C_9H_6 (**5**); M = Mo, Ind' = 1-(C_9H_6N)C_9H_6 (**6**) a M = W, Ind' = 1-(C_9H_6N)C_9H_6 (**7**), were obtained in moderate isolated yields 59–67 %.

Table 1 Selected infrared data of compound **4**–**12**.

	ν_a^{CO} (cm^{-1})	ν_s^{CO} (cm^{-1})	ν^{BF} (cm^{-1})
4	1938	1860	–
5	1924	1833	–
6	1933	1854	–
7	1927	1844	–
8	1971	1889	1054
9	1937	1850	1076
10	2021	1942	1056
11	2021	1942	1056
12	2003	1869	1055
13	2020	1939	1058
[(η^5-C_9H_7)(η^3-C_3H_5)Mo(CO)$_2$] [23]	1963	1887	–
[[(η^5-C_9H_7)Mo(CO)$_2$(NCCH$_3$)$_2$][BF_4] [24]	1970	1880	–

The compounds **4**–**7** are yellow crystalline materials well soluble in polar organic solvents and aromatic hydrocarbons. The characterization using ^{1}H and ^{13}C NMR spectroscopy revealed two isomeric complexes with *supine*- and *prone*- allyl in solution easily distinguished by considerable upfield shifted protons of the allyl due to the indenyl diatropic ring current effect which is characteristic for the complexes of type [(η^5-Ind')(η^3-allyl)M(CO)$_2$].[25] The infrared spectrum of compound **2** shows two carbonyl stretching bands in the range typical for terminal carbonyl ligands (Table 1). The wavenumbers are comparable with those reported for parent indenyl complex [(η^5-C_9H_7)(η^3-C_3H_5)Mo(CO)$_2$][26] suggesting a negligible effect of the indenyl modification on electron density on molybdenum atom (**Table 1**). The complexes **4**–**7** were characterized by X-ray diffraction (Figure 1). The single-crystals suitable for the analysis were obtain by slow cooling of saturated complex in hexane. The X-ray data confirm the absence of interaction between donor atom from substituted indenyl and molybdenum or tungsten. Thus, the η^3-allyl, η^5-indenyl and two carbonyls adopt pseudo-tetrahedral environment around the molybdenum atom. Hapticity of the indenyl in crystal structure was quantified using structural parameter Δ(M–C) and envelop fold angle Ω. Low values of Δ(M–C) [0.109(17) Å] and Ω [4.4(2)°] prove η^5-coordination mode with a small contribution of η^{3+2} that is typical for η^5-indenyl molybdenum complexes of.[24,27]

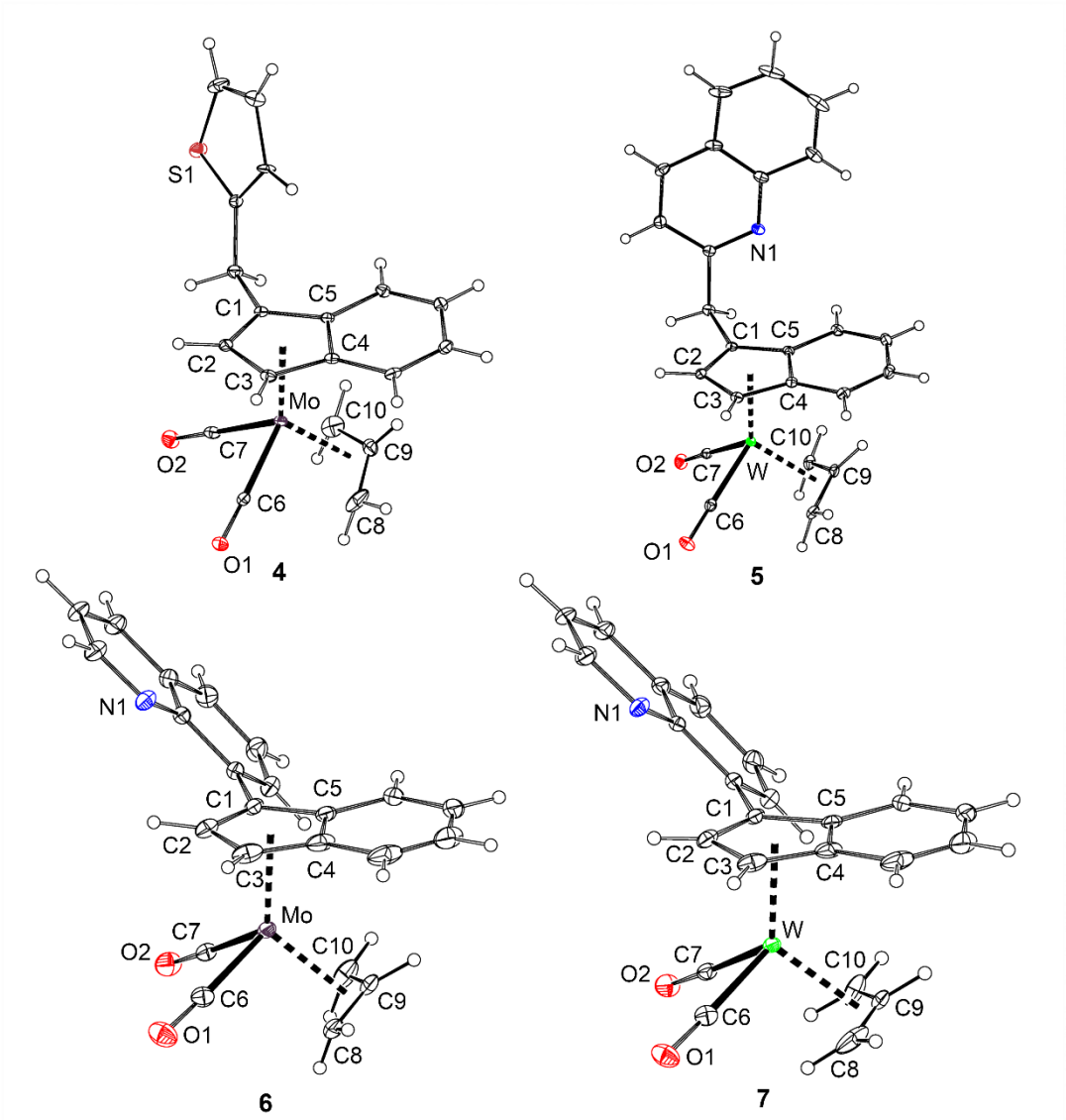

Figure 1 Crystal structures of complexes **4**–**7**.

Table 2 Selected bond lengths (Å) and angles (°) for compounds **4**, **6** (M = Mo) and **5**, **7** (M = W).

	4	**5**	**6**	**7**
M–Cg1 [a]	2.0303(8)	2.0293(12)	2.028(2)	2.0303(8)
M–Cg2 [a]	2.0441(15)	2.028(3)	2.031(5)	2.0314(10)
M–C6	1.9541(17)	1.943(5)	1.951(5)	1.9472(17)
M–C7	1.9436(17)	1.933(2)	1.943 (5)	1.9396(17)
C6–M–C7	80.8(7)	81.32(10)	80.8(2)	81.74(7)
Cg1–M–Cg2 [a]	128.2(5)	127.95(9)	125.69(14)	125.91(4)

[a] Cg1 is centroid of the five-membered ring of the indenyl, Cg2 is centroid of the allyl

4.3 Protonation of the allyl ligand

In the next step, the reaction of complexes **4**–**7** with strong acid was studied. For the analogous reaction with compound [(η^5-Cp)(η^3-allyl)Mo(CO)$_2$], the highly labile η^2-propen product with Mo–FBF$_3$ was proposed.[28] Since compounds **4**–**7** contains donor atom in the side chain, the weakly bonded BF_4^- would be exchanged for the intramolecular coordination leading to stabilization of η^2-propene complex. Thus, to obtain such a species, the reaction of **4**–**7** with HBF$_4$·Et$_2$O was carried out at low temperature and non-coordinating solvent (CH_2Cl_2). The most important aspect of the studied protonation reaction is that the substitution of the indenyl ligand considerably affect the formed product.

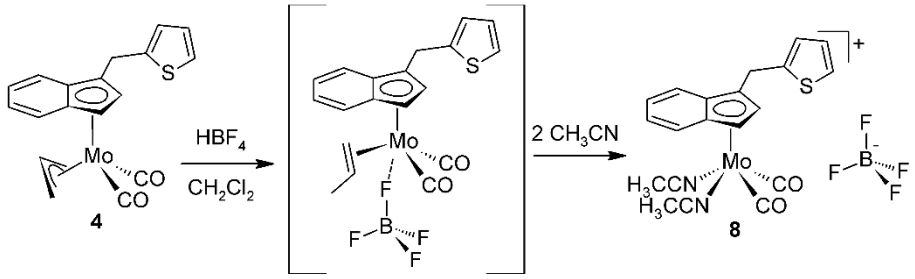

Scheme 4 Protonation of complex **4**.

The reaction of **4** with fluoroboric acid, within aforementioned conditions, leads to rapid color change from yellow to dark red, which suggest successful protonation of the allyl. Nevertheless, attempts to isolate the formed species in solid state, by slow evaporation of solvent at low temperature or by recrystallization using precooled Et$_2$O, was unsuccessful due to decomposition of the complex. The compound was studied by NMR tube reaction and slow warning of the sample from –30 °C to 0 °C revealed liberation of free propene (δ = 1.69, 4.89, 5.79 ppm) whose NMR data was described in literature.[29] This instability is rather typical for the aforementioned complex with unsubstituted Cp ligand[28] [(η^5-Cp)(η^2-propene)Mo(CO)$_2$FBF$_3$], suggesting that desired S → Mo interaction is not formed. To confirm this hypothesis and trap species without intramolecular coordination, the reaction of labile η^2-propene compound with two equivalents of CH_3CN were performed. As a result the stable and easily isolable complex [{η^5-1-($C_4H_3SCH_2$)C_9H_6}Mo(NCCH_3)$_2$(CO)$_2$][BF_4] (**8**) is formed (**Scheme 4**). ^{1}H NMR spectrum of the final product **8**, measured in CD_2Cl_2, revealed resonances of two coordinated acetonitrile ligands, which appear at considerably lower-field (2.47 and 2.41 ppm) than free acetonitrile (1.97 ppm).[29] Chemical shifts of indenyl protons H^{2,3} (5.14 and 5.99 ppm)and *ipso*-carbons (119.1 and 119.8 ppm) confirm its η^5-coordination mode. Two ^{13}C resonances at 248 and 247 ppm evidence the presence of two carbonyl ligands in the coordination sphere of **8**. As usual for molybdenum carbonyl complexes,[27,30,31] the proposed solution structure of **8** satisfies 18-electron rule. Thus, S→Mo interaction was excluded despite the accessible lone pairs located on sulfur atom. IR spectrum of **8** shows two carbonyl stretching bands shifted significantly to higher energies compared to the vibration modes of **4**. Such observation, together with typical broad B–F vibration band of BF_4^- at 1054 cm^{-1}, confirms successful protonation and exchange of negatively charged allyl and appearance of the cationic complex. Moreover, the wavenumbers of carbonyl vibration bands are practically identical with

those described for parent $[(\eta^5\text{-}C_9H_6)Mo(CO)_2(NCMe)_2][BF_4]$,[24] giving further relevant evidence that thiophene function is not involved in the donor-acceptor interaction with the central metal.

Next, the complex **5** was, analogously protonated with $HBF_4{\cdot}Et_2O$, using the same protonation protocol. In this case, the yellow precipitate was formed within the stirring of the reaction mixture overnight at −30 °C. In this case, the quantitative protonation of the indenyl side chain takes place and complex $[(\eta^3\text{-}C_3H_5)\{\eta^5\text{-}1\text{-}(C_9H_6NHCH_2)C_9H_6\}W(CO)_2][BF_4]$ (**9**) was formed (**Scheme 5**).

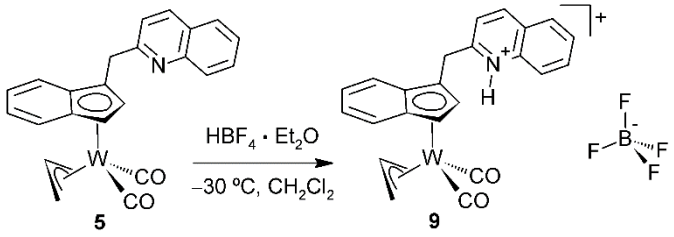

Scheme 5 Protonation of complex **5**.

Similarly as in the case of **5**, the ^1H and ^{13}C NMR spectra of **9** show two sets of resonances corresponding to *exo*- and *endo*- conformers. With exceptions of two broad signals at 13.3 and 14.2 ppm, the pattern of the ^1H NMR spectra of **9** is analogous to **5**. The highly low-field shifted signals were assigned to N*H* protons of two conformers, which confirms the protonation of nitrogen atom. Moreover, the wavenumbers of carbonyl valence vibrations have similar values as described for **5** (**Table 2**), which confirm that the electron density of central metal is not affected by the protonation of the allyl ligand.

The dark red solution is formed upon mixing of **6** and **7** with $HBF_4{\cdot}Et_2O$ in CH_2Cl_2 at −30°C. Upon slow warming of the solutions up to room temperature significant darkening of the mixtures were observed and the chemical shift of ^1H NMR signals of propene match well with values described for free propene (δ = 1.69, 4.89, 5.79 ppm).[29] Nevertheless, slow precipitation with Et_2O (also precooled to −30 °C) afforded complexes $[\{\eta^5\text{:}\kappa N\text{-}1\text{-}(C_9H_6N)C_9H_6\}(\eta^2\text{-}C_3H_6)Mo(CO)_2][BF_4]$ (M = Mo (**10**), W (**11**)) as orange crystals in excellent yield (~95%). In case of tungsten complex, the crystals of **11** could be stored for a few weeks at room temperature but molybdenum analogue **10** is significantly less stable and must be kept at low temperature even in the solid state.

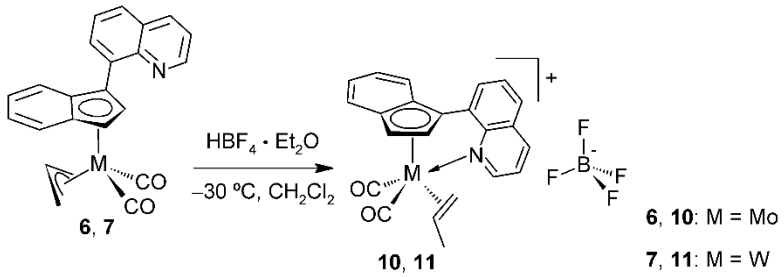

Scheme 6 Synthesis of propene complexes **10** and **11**.

The compounds **10** and **11** were characterized by multinuclear NMR spectroscopy (measured at −30°C) as their CD_2Cl_2 solutions. The ^1H NMR spectrum revealed one set

of sharp signals. Particular attention was given to the upfield area of the spectra displaying three signals with the integral intensity ratio of 2:1:3. The signals are up to 3 ppm upfield shifted compared to free propene suggesting the formation of the bond between the alkene and transition metal. ^{13}C chemical shifts of propene carbons are even more appreciable as CH carbon is up to 80 ppm upfield shifted. Important aspect of the propene protons signals in ^{1}H NMR spectra is a considerable lowering of the *J*-values compared to the free propene (**Table 3**). This is connected with relatively strong π-back bonding between central metal and alkene ligand, which lead to the contribution of sp^3 hybridization on propene carbons bonded to metal.

Table 3 Values of the chemical shift (δ), multiplicity (m) and interaction constants (*J*) for the signals of free propene and coordinated in the case of **10** and **11**.

	δ_{CH_3} (m; *J*) [a]	δ_{CH} (m; *J*) [a]	δ_{CH_2} (m; *J*) [a]	
10	1.16 (d; 5,6)	2.76 (ddq; 14,5; 9,1; 5,6)	2.87 (dd; 9,1; 4,8)	3,32 (dd; 14,5; 4,8)
11	1,24 (d; 5,6)	1,99 (ddq; 16,6; 12,5; 5,6)	2,58 (dd; 12,5; 6,6)	2,61 (dd; 16,6; 6,6)
C_3H_6 [b]	1,69 (dt; 6,4; 1,5)	5,79 (m)	2,87 (dm; 10)	3,32 (dm; 17)

[a] values of δ are in ppm, *J* in Hz
[b] values for free propene were found in literature[29]

The ^{19}F NMR and ^{11}B NMR spectra revealed sharp signals at around –151.0 and –1.4 ppm, respectively. These values are typical for symmetrical BF_4^- anion. Thus, in case the of **3** and **4**, the NMR spectroscopy clearly exclude M←F–BF_3 interaction, which was previously suggested for [(η^5-Cp)(η^2-C_3H_6)Mo(CO)$_2$(FBF_3)].[1] This observation is further supported by IR spectrum displaying B–F stretching modes as relatively narrow, symmetrical bands at 1056 (**10**) and 1059 cm^{-1} (**11**), which is also typical for tetrahedral BF_4^- counter anion. Considerably upfield shifted resonances (~110 ppm) of indenyl carbons C^{3a} and C^{7a} reveal η^5-coordination mode of the indenyl, which well correlates with ^{1}H NMR pattern of protons H^2 (~6.0 ppm) and H^3 (~6.5 ppm). We note that intramolecular N→M interaction is expected for **10** and **11** as group 6 metal carbonyl complexes usually satisfy 18e valence rule. In the case of **11**, the proposed structure was confirmed by single-crystal X-ray diffraction analysis (Fig. 2). The coordination sphere of the tungsten atom adopts a distorted square pyramidal geometry. The η^5-indenyl occupies the apical position whereas basal plane contains two carbonyls in the *cis* arrangement, nitrogen atom from quinoline and η^2-coordinated propene. The benzannulated moiety of indenyl is not located *trans* to carbonyl ligands as usual for the complexes containing [(η^5-Ind)M(CO)$_2$] fragment [3,4,6,24,32] but above propene ligand and neighboring carbonyl. Such an unprecedented structure motif is enforced by rigid N→W intramolecular coordination.

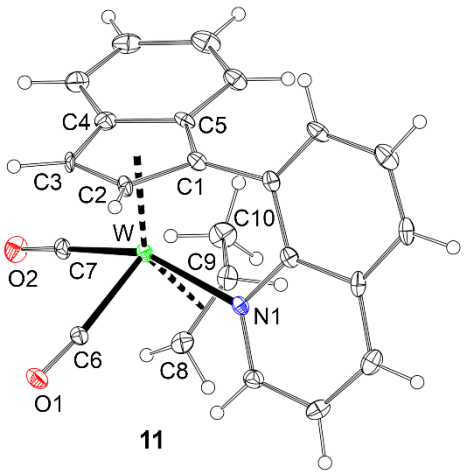

Figure 2 Crystal structure of **11**. Selected bond lengths (Å) and angles (º): Cg(Cp)–W = 2.010(1), W–N1 = 2.2747(7), C8–C9 = 1.409(16), C6–W = 2.044(9), C7–W = 1.994(10), C8–W = 2.287(8), C9–W = 2.280(9), Cg(C_3H_6) = 2.172(10), C6–W–C7 = 81.5(3), Cg(C_3H_6)–W–Cg(Cp) = 140.4(2).

The propene C=C bond, with the interatomic distance of 1.409(16) Å, is significantly longer compared to free ethylene 1.337(2) Å.[33] The elongation, rising up due to donation from π^b and into π^a of the propene, is considerably greater than described for Zeise's salt but is rather typical for low-valent or electron-rich alkene complexes of early and middle transition metals such as [(η^5-Cp')$_2$(η^2-C_2H_4)Ti] [$d_{C=C}$ = 1.454(9) Å], [(η^5-Cp)(η^2-C_2H_4)Nb(C_2H_5)] [$d_{C=C}$ = 1.406 (13) Å] or [(η^2-C_2H_4)$_2$Mo(PDI)] [$d_{C=C}$ = 1.421(6) and 1.379(6) Å, respectively], where DPI is 2,6-(2,6-(*i*Pr)$_2$$C_6H_3$N=CCH$_3$)$_2$$C_5H_3$N.[34–36] It could be noted that methyl group of η^2-propene is displaced out of double bond plane (which is perpendicular to the plane defined by W, C21 and C22 atoms) by 24.5(11)°, which further supports a considerable contribution of π-back donation and the overall structure could be rather described as a metallacycle.

4.4 Reactivity of propene complexes

In order to examine a possible exchange of the coordinated propene, the reactivity of **10** and **11** toward various monodentate ligands was studied. The complexes react with dimethyl sulfide (dms) to afford dark red solutions giving, after workup, bright red crystals of [{η^5:κ*N*-1-(C_9H_6N)C_9H_6}M(CO)$_2$(SMe_2)][BF_4] (**12**: M = Mo, **13**: M = W; **Scheme 7**). The successful propene exchange was evidenced by multinuclear NMR spectroscopy. The upfield part of ^{1}H NMR spectrum displays a new signal with a chemical shift 2.08 ppm, which was assigned to one molecule of coordinated dms. The downfield area shows a very similar pattern as described for **10** and **11**, implying η^5-coordination mode of the indenyl.

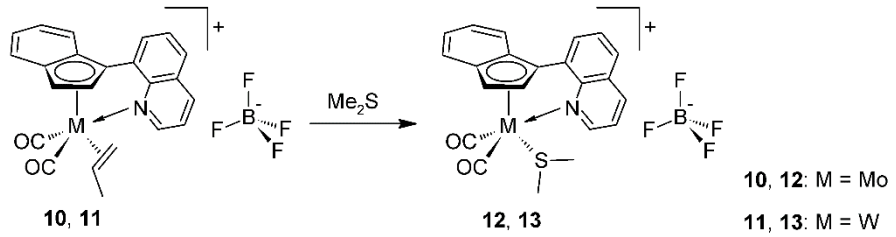

Scheme 7 Synthesis of dms complexes **12** and **13**.

Infrared spectra also confirmed the propene exchange as the carbonyl stretching bands are shifted to lower wavenumbers compared to **10** and **11** (**Table 1**). Despite the significant shift, the stretching bands of **12** and **13** have still relatively high energy compared, for example, with the previously reported complex with intramolecular coordination $[(\eta^5{:}\kappa N\text{-}C_5H_4NCH_2C_5H_4)Mo(CO)_2(NCCH_3)][BF_4]$ containing CH_3CN ligand instead of dms (1982 and 1866 cm^{-1}) . This could be attributed to the ability of dms to act as the π-acid, which is a property previously described for several organosulfur ligands, including thioethers.[3,37] In the case of **12**, the slow diffusion of Et_2O into a saturated CH_2Cl_2 solution gives single-crystals suitable for X-ray diffraction analysis (Fig. 2). Although several dimeric Cp molybdenum complexes with bridging dms ligand were previously described in the literature,[38,39] the **12** is, to our best knowledge, the first example of fully structurally characterized indenyl compounds with dms acting as a simple monodentate ligand. The coordination polyhedron adopts distorted square pyramidal geometry, similarly as in the case of **4**, with η^5-indenyl in apical position and carbonyls, nitrogen and sulfur donors in the basal plane. The dimethyl sulfide is bonded to molybdenum through one of the lone pairs leading to low values of C–S–Mo angles [109.29(10), 113.50(8) Å], which is typical for molybdenum or late-transition metals coordination complexes of dms.[40,41] The Mo–S bond length [2.5118(6) Å] is significantly longer than reported Pt–S bonds (typically ~2.25 Å).[40] On the other hand, the structurally characterized molybdenum dms coordination complexes, e.g., $[MoCl_5(Me_2S)]^-$ or $[MoCl_4(Me_2S)_2]$ have analogously long Mo–S distance [2.5538(19) and 2.5297(6) Å respectively].[41] This seems to be a consequence of the less thiophilic character of the molybdenum(II) compared to late transition metals. Weaker M–S bond is also evident from slightly shorter (~0.01 Å) S–C bonds as the smaller contribution of π-back donation is related with the lower occupation of the σ-orbitals antibonding to C–S bonds.

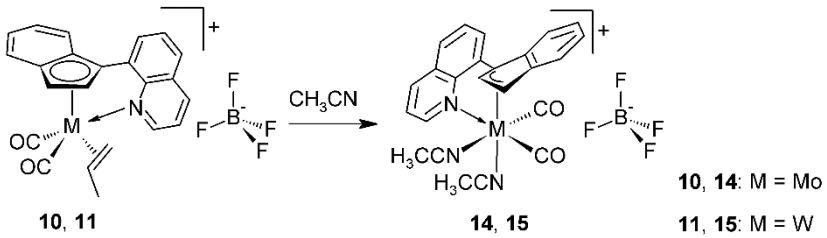

Scheme 8 Reactivity of **10** and **11** toward CH_3CN.

The propene complexes **10** and 11 readily react with acetonitrile to afford $[\{\eta^3{:}\kappa N\text{-}1\text{-}(C_9H_6N)C_9H_6\}M(CO)_2(NCCH_3)_2][BF_4]$ (**14**: M = Mo, **15**: M = W; **Scheme 8**). Although the reaction is not accompanied by significant color change, our NMR experiments in CD_3CN proved full conversion within a few minutes even at –30°C. The

propene exchange is accompanied with coordination of second acetonitrile molecule inducing the haptotropic $\eta^5 \rightarrow \eta^3$ rearrangement of the indenyl ligand as confirmed by multinuclear NMR spectroscopy. The η^3-coordination mode of the indenyl ligand is recognized from downfield shifted carbons $C^{3a/7a}$ and protons H^2 (~150 ppm in ^{13}C and 7.52, 6.73 ppm in ^1H NMR) compared to **10** and **11**. The cleavage of π-acidic alkene was also confirmed by infrared spectroscopy since CO stretching bands are ~30 cm^{-1} shifted to lower energies due to considerably weaker π-accepting properties of CH_3CN ligands. Such spectral data well matches to X-ray diffraction analysis of **15** that confirms the distorted octahedral structure with η^3:κ*N*-bonded 1-(quinol-8-yl)indenyl, two *cis*-coordinated carbonyls and two *cis*-coordinated acetonitrile ligands (Fig. 3).

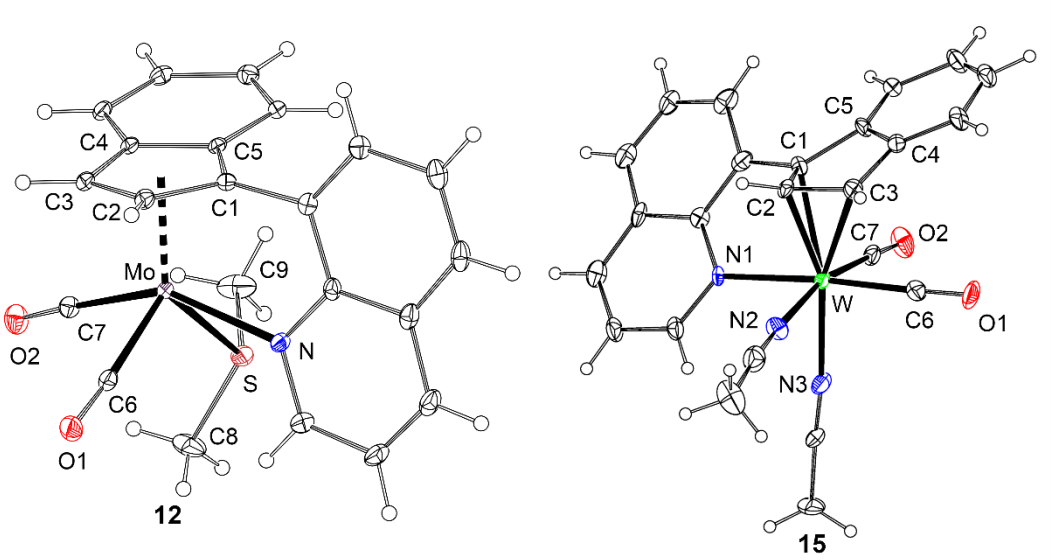

Figure 3 Crystal structure of cations **12** and **15**. Selected bond lengths (Å) and angles (º): **12**: Cg(Ind)–Mo = 2.0094(9), Mo–N = 2.252(2), Mo–S = 2.5118(6), Mo–C6 = 1.937(2), Mo–C7 = 2.034(2), C6–Mo–C7 = 82.03(9), Cg(Ind)–Mo–S = 130.80(8), C8–S–Mo = 109.29(10), C8–S–Mo = 113.50(8).

4.5 Acetonitrile ligand exchange

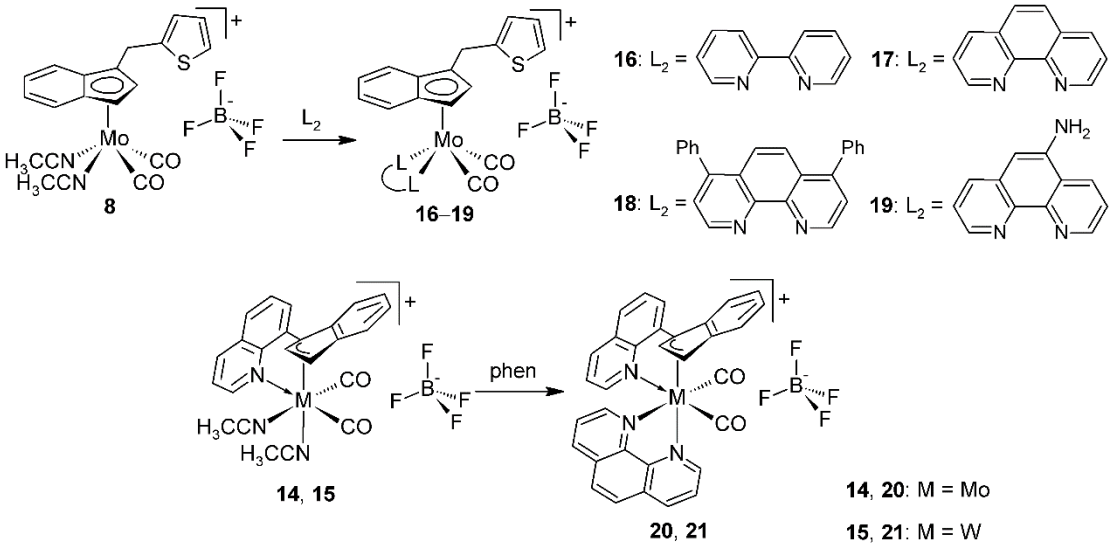

Scheme 9 Acetonitrile ligand exchange.

For the complexes [{η^5-1-($C_4H_3SCH_2$)C_9H_6}Mo($NCCH_3$)$_2$(CO)$_2$][BF_4] (**8**) a [{η^3:κ*N*-1-(C_9H_6N)C_9H_6}M(CO)$_2$($NCCH_3$)$_2$][BF_4], where M = Mo (**14**), W (**15**) the reactivity toward various *N*,*N*-chelating ligands were studied (**Scheme 9**). As expected, acetonitrile ligands of **3** are readily exchanged by various of these proligands, including 1,10-phenanthroline (phen), 4,7-diphenyl-1,10-phenanthroline (Ph_2phen), 1,10-phenanthroline-5-amine (NH_2phen) or 2,2'-bipyridine (bpy). In the case of **8**, the reactions give [{η^5-1-($C_4H_3SCH_2$)C_9H_6}ML_2(CO)$_2$][BF_4], where L_2 = bpy (**16**), phen (**17**), Ph_2phen (**18**), NH_2phen (**19**). On the other hand, the reaction of **14** and **15** with phen gives [{η^3:κ*N*-1-(C_9H_6N)C_9H_6}M(CO)$_2$(phen)][BF_4], where M = Mo (**20**), W (**21**). The complexes were characterized using ^{1}H and ^{13}C{^{1}H} APT NMR spectroscopy. Whereas for **16**–**19**, due to the absence of S → Mo interaction, the indenyl remains η^5-bonded to central metal, in case of **20** and **21,** the fragment [{η^3:κ*N*-1-(C_9H_6N)C_9H_6}M(CO)$_2$] is unchanged. Moreover, the low-field are of ^{13}C and ^{1}H NMR spectra of **16**–**21** show signals of appropriate *N*,*N*-chelates. The number of signals corresponds to expected number for the ligand in point group of symmetry C_1, confirming the coordination to central atom. IR spectra of **16**–**21** showed two carbonyl stretching bands slightly shifted to lower energies compared to **8**, **14** and **15**. The shift can be rationalized through somewhat stronger σ-donating ability of the bidentate ligands compared to the acetonitrile, further confirming the presence of *N*,*N*-chelating ligand in the coordination sphere of **16**–**21**.

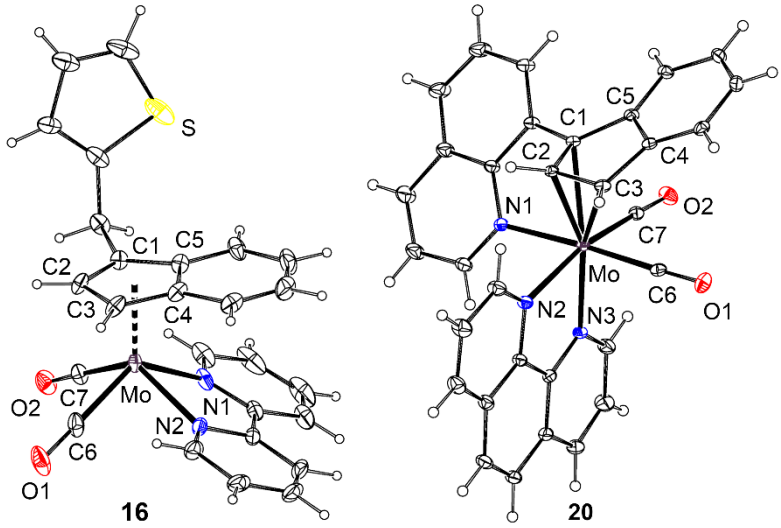

Figure 4 Crystal structures of cations **16** and **20**. Selected bond lengths (Å) and angles (º): **16**: Cg(Cp)–Mo = 2.3041(9), C6–Mo = 1.986(2), C7–Mo = 1.976(2), N1–Mo = 2,2605(18), N2–Mo = 2,2709(17), N3–Mo = 2,1938(16), Cg(Cp)–Mo–N3 = 171,6(5), C6–Mo–C7 = 82,89(9), N1–Mo–N3 = 86,06(6); **18**: Cg(Cp)–Mo = 1,9965(17), C6–Mo = 1,970(3), C7–Mo = 1,962(3), N1–Mo = 2,190(3), N2–Mo = 2,183(3), C6–Mo–C7 = 73,3(1), N1–Mo–N2 = 72,8(1).

The solid-state structure of the compound **16** and **20** was determined by the single-crystal X-ray diffraction analysis (**Figure 4**). Selected bond distances and bond angles are listed in the caption of **Figure 4**. The coordination sphere of **16** around central molybdenum adopts distorted square-pyramidal molecular geometry with indenyl in the apical position. The basal plane contains two *cis*-arranged carbonyls and nitrogen donors

of 2,2'-bipyridine. The bidentate ligand is located below the annulated benzene ring of the indenyl representing most common conformation of indenyl complexes of the type $[(\eta^5\text{-Ind'})Mo(CO)_2L_2]^+$ reported for various chelates so far.[3,6,24,27] For complex **20**, the coordination sphere adopts pseudo-octahedral geometry. Analogously as in the case of **15**, the centroid of η^3-indneyl and two carbonyls adopt *fac*-configuration and nitrogen donor of the quinoline is located *trans* to one of the CO ligands. The remaining two positions are occupied with nitrogen atoms of the phen ligand.

4.6 Quantum-chemical calculations

The bis(acetonitrile) complexes with intramolecular N → M coordination $[\{\eta^3{:}\kappa N\text{-}1\text{-}(C_9H_6N)C_9H_6\}M(CO)_2(NCCH_3)_2][BF_4]$, where M = Mo (**14**), W (**15**) exhibit unusual stable η^3-bonded indenyl without tendency to backward $\eta^3 \rightarrow \eta^5$ switch in coordinating (CH_3CN) or non-coordinating (CH_2Cl_2) solvent. This is surprising, especially considering rapid dynamic behavior at room temperature (**Scheme 10**), described previously for the system $[(\eta^3\text{-Ind})Mo(NCCH_3)_3(CO)_2][BF_4]$ (**A**) ↔ $[(\eta^5\text{-Ind})Mo(NCCH_3)_5(CO)_2][BF_4]$ (**D'**).[2]

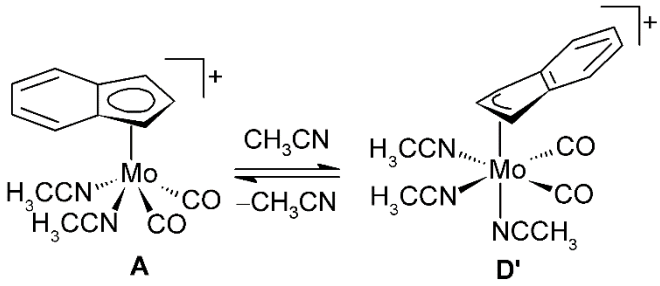

Scheme 10 Dynamic haptotropic rearrangement at room temperature.

To bring insight into the unusual stability of η^3-coodination mode in the case of **14**, the series of quantum-chemical calculations were performed. In the first step, the selected level of theory (DFT/B3LYP/cc-pVDZ-PP) was compared to the XRD data (**Figure 5**). For this purpose, the complex **16** and cation $[(\eta^5\text{-Ind})Mo(NCCH_3)_2(CO)_2]^+$ (**D'**), whose crystal structure[24] was published previously, were used. The root mean square deviation (RMSD) of the calculated and XRD sets of coordinates have low values of ~0.1 Å confirming good match of the experimental data with theoretical ones.

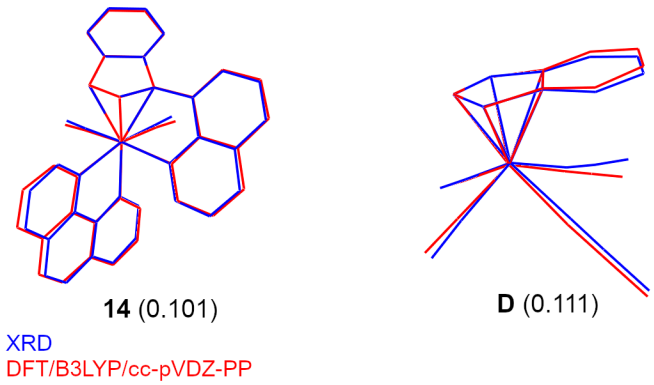

Figure 5 Superposition of calculated and XRD sets of coordinates. RMSD in brackets is given in Å.

Next, the energy profile of haptotropic rearrangement of the system [(η^3-Ind)Mo(NCCH$_3$)$_3$(CO)$_2$][BF$_4$] (**A**) ↔ [(η^5-Ind)Mo(NCCH$_3$)$_5$(CO)$_2$][BF$_4$] (**D'**) was calculated (**Figure 6**). The most stable species of the whole profile is compound **A** and all electronic energies are related to thus compound. On the other hand, the most stable species with η^5-indenyl is **D'**. The equilibrium between these two complexes, which was proved in previous study,[2] suggest that the rotation of indenyl ligand is important factor of the haptotropic rearrangement. The calculated ring slippage from **A** to corresponding η^5 species exhibit to high activation energy (E_A) to be allowed at room temperature. Nevertheless, analogous rearrangements for complexes with indenyl ~90º (**B**) and ~180º (**C**) rotated revealed considerable lowering of the E_A values. This means, that for the system [(η^3-Ind)Mo(NCCH$_3$)$_3$(CO)$_2$][BF$_4$] (**A**) ↔ [(η^5-Ind)Mo(NCCH$_3$)$_5$(CO)$_2$][BF$_4$] (**D'**), the activation energy of indenyl ring slippage is affected by position of π-ligand toward [Mo(CO)$_2$] fragment.

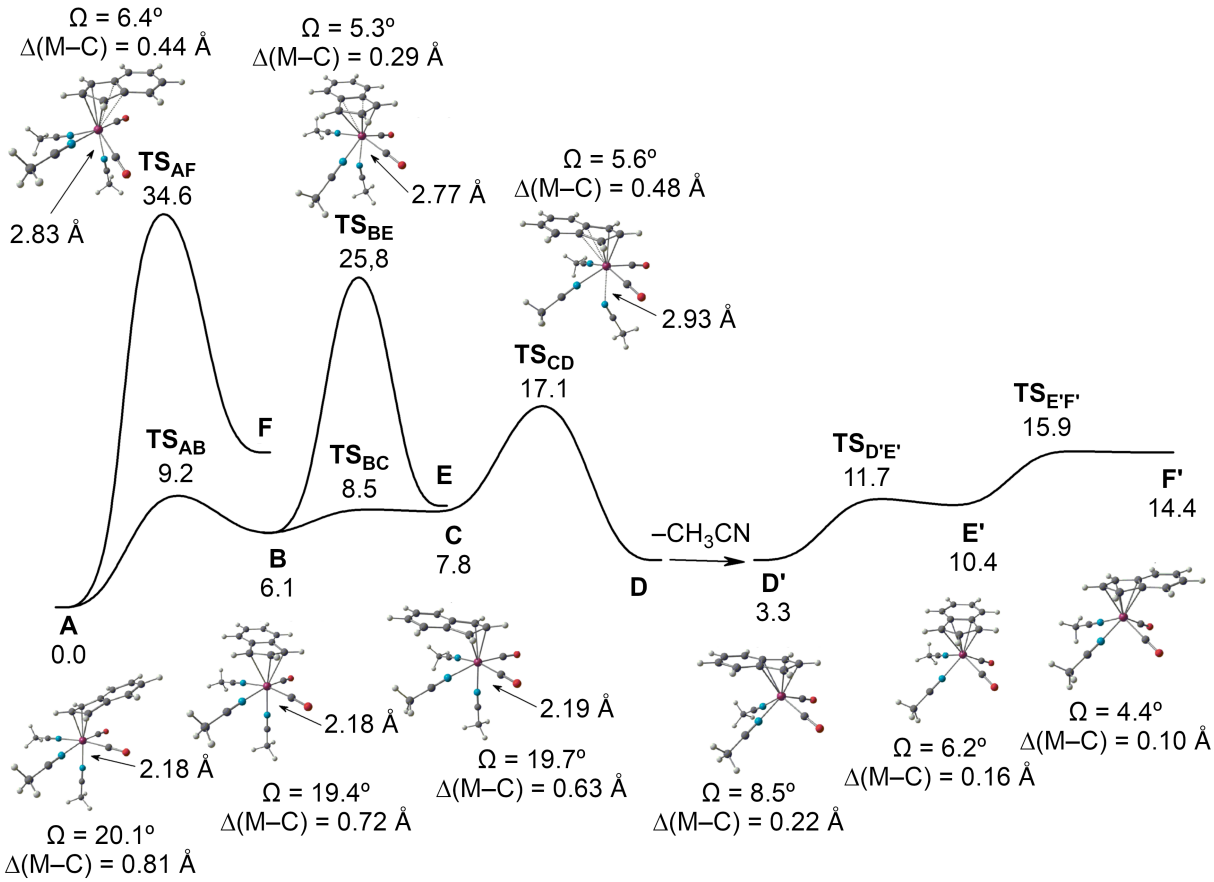

Figure 6 Energetic profile of haptotropic rearrangement for complex [(η^3-Ind)Mo(NCCH$_3$)(CO)$_2$]$^+$. The electronic energies are given in kcal/mol.

The highest E_A values exhibit the aforementioned hapticity switch **A** → **F'** (34.6 kcal/mol) a during the rotation of indenyl this value decreases up to lowest values of 17.1 kcal/mol (**D** → **E'**) and this ring slippage is allowed at room temperature. Moreover, the energy profile in the **Figure 6** shows calculated rotational barriers of the indenyl. All these barriers have values lower than 10 kcal/mol. Thus, the rotation might easily take place at room temperature as well. In the case of complexes with intramolecular coordination, the overall situation is highly affected by the strong

intramolecular coordination. For the η^2-propene complex, the reaction with CH_3CN unambiguously gives η^3-indenyl compound **14**. Importantly the **10** and **14** have opposite configuration of indenyl toward $[Mo(CO)_2]$ fragment, meaning that the reaction with CH_3CN is accompanied by the change of this configuration. Unfortunately, this reaction is rapid and we were not able to trap any intermediate with η^5-indenyl and one coordinated molecule of CH_3CN, even using NMR tube reaction at low temperature. Nevertheless, one might expect the analogous species as a dms complex **12** is formed in the first step and subsequently, another molecule of CH_3CN induces the ring slippage **14-D'** → **14-C** (**Figure 7**). This rearrangement is allowed at room temperature, since **14-D'** is the same conformer as **D'** (**Figure 6**) with low value of the E_A.

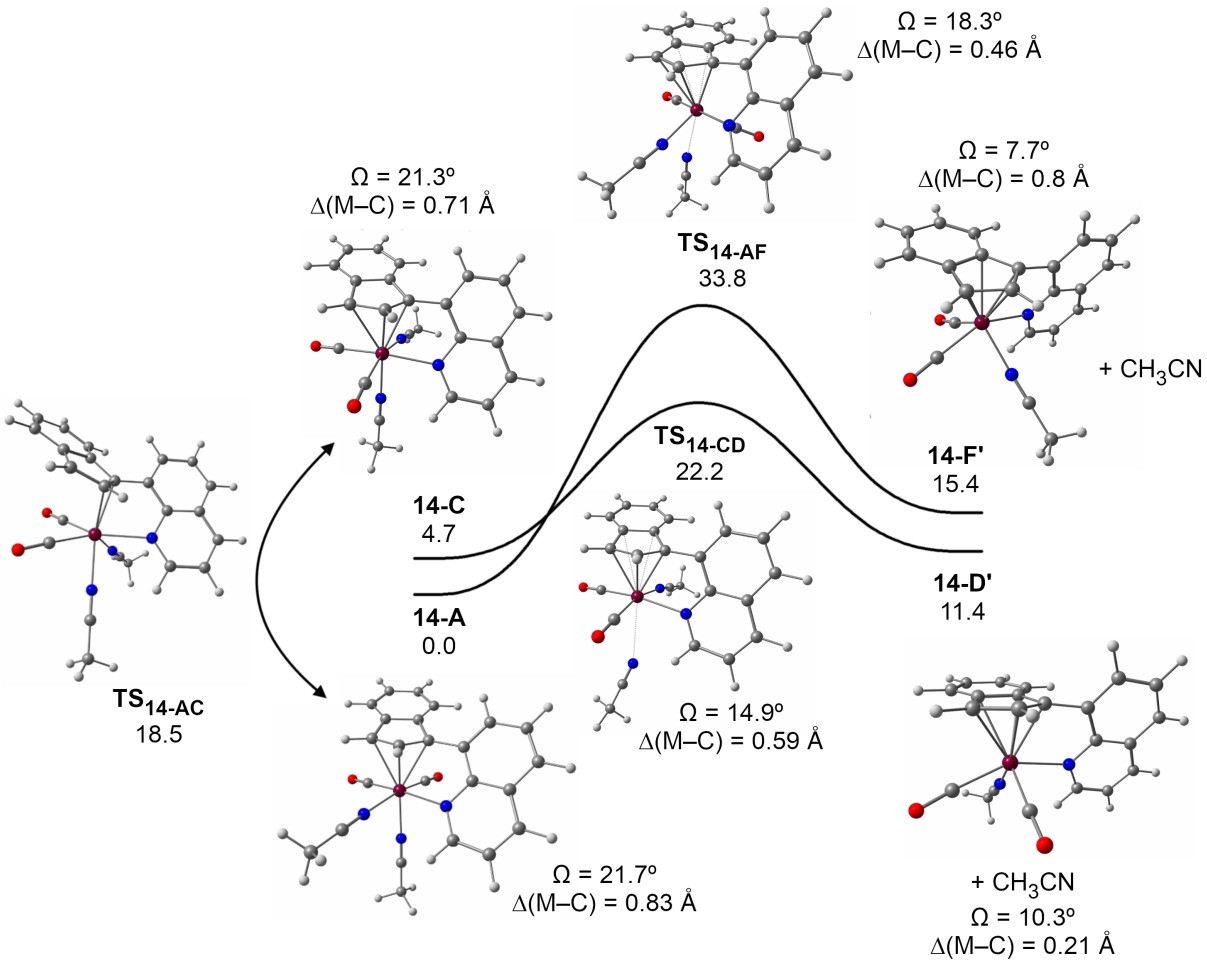

Figure 7 Calculated energy profile for haptotropic rearrangement of synthesized compound **14**. Electronic energies are given in kcal/mol.

The existence of **14-A** in solution and solid phase was fully experimentally proved. However, the remaining question is what the mechanism of changing conformation from **14-C** to **14-A**. The rotation of indenyl might be excluded due to strong N → Mo intramolecular coordination. From the mechanistic point of view, several mechanisms of changing the conformation could be considered as relevant. (A) Change of the configuration within dissociative/associative exchange of the CH_3CN. The acetonitrile has generally weak coordination properties and it could be easily exchange for another molecule of CH_3CN. This process was proved by ^1H NMR spectroscopy, where exchange of the CH_3CN for CD_3CN was observed. Nevertheless,

the calculated profiles show that the change of conformation, induced by dissociation/association of CH_3CN, cannot take place due to large activation energies of this process. If the switch to another conformer was enforced by geometrical constraints, the dissociation of $N \rightarrow Mo$ intramolecular coordination was observed within the optimization of energy profile, which is not in line with experimental results. (B) the second mechanism is based on Berry pseudorotation (BPR). The classical BPR is based on intra-conversion of ligand in case of the trigonal bypiramidal (D_{3h}) polyhedron, which goes through tetragonal pyramidal (C_{4v}) transition state.[42,43] Recently, the modified BPR where octahedral transition states were described in literature.[44] Similarly, for the **14-A** and **14-C**, the calculation suggested possible change of conformation using the BPR. Although the appropriate TS has relatively high activation barrier of 18.5 kcal/mol, this process is allowed at room temperature.

As already mentioned above, the species **14-A** was experimentally proved and $\eta^3 \rightarrow \eta^5$ switch was not observed. This might be explained by following aspects. (A) the reverse $\eta^3 \rightarrow \eta^5$ ring slippage is not allowed due to high values of E_A (33.8 kcal/mol). This match well with the profile for the compound with unsubstituted indenyl (**Figure 6**). (B) Although, the backward BPR to afford **14-C** and subsequent $\eta^3 \rightarrow \eta^5$ rearrangement to afford **14-D'** is allowed at room temperature, this process does not take place due to significant energetic difference between **14-A** and **14-D'** (11.5 kcal/mol).

5 Conclusion

In this combined experimental/theoretical work, the 18 new organometallic compounds were synthesized and characterized. The main aim of this thesis is to evaluate the impact of a strong intramolecular coordination on the hapticity of indenyl ligand. Thus, in the first step, two new derivatives of indene, 3-($C_4H_3SCH_2$)C_9H_7 (**1**) a 3-($C_9H_6NCH_2$)C_9H_7 (**2**), were designed and synthesized while the congener 3-(C_9H_6N)C_9H_7 (**3**) was prepared according to the procedure described in the literature. The pro-ligands **1**–**3** were subsequently used for the syntheses of mixed allyl/indenyl complexes [(η^3-C_3H_5)(η^5-Ind')M(CO)$_2$], where M = Mo, Ind' = 1-($C_4H_3SCH_2$)C_9H_6 (**4**); M = W, Ind' = 1-($C_9H_6NCH_2$)C_9H_6 (**5**); M = Mo, Ind' = 1-(C_9H_6N)C_9H_6 (**6**) a M = W, Ind' = 1-(C_9H_6N)C_9H_6 (**7**). These compounds were fully characterized using multinuclear NMR an IR spectroscopy and X-ray diffraction. In the next step, the protonation reaction of **4**–**7**, using $HBF_4 \cdot Et_2O$ in CH_2Cl_2 at –30 ºC, was studied in detail. For compound **4** the reaction leads to allyl protonation and cleavage (after the addition of CH_3CN) but desired S → Mo intramolecular coordination was not observed. In the case of **5**, the reaction with one equivalent of $HBF_4 \cdot Et_2O$, within the condition mentioned above, gives quantitatively species with the protonated side chain of the indenyl [(η^3-C_3H_5){η^5-1-($C_9H_6NHCH_2$)C_9H_6}W(CO)$_2$][BF_4] (**9**). Finally, for the complexes **6** and **7**, the protonation afforded the desired motif with intramolecular N → M interaction and the compounds [{η^5:κN-1-(C_9H_6N)C_9H_6}(η^2-C_3H_6)M(CO)$_2$][BF_4] [M = Mo (**10**) a W (**11**)] were formed. It was found, that strong intramolecular coordination stabilizes fragment with η^2-bonded propene, and therefore, the complexes **10** and **11** are easily isolable in a solid-state. Moreover, for **11**, the suggested structure was proved by X-ray diffraction, and to our best knowledge, this is the first unambiguous prove, that the alkene compounds are formed within the protonation of complexes of the type [(η^5-Cp')(η^3-allyl)M(CO)$_2$]. In the next step, the reactivity of propene complexes **10** and **11** was studied. The reaction of these complexes with dimethyl sulfide (dms) gives compounds [{η^5:κN-1-(C_9H_6N)C_9H_6}M(CO)$_2$(dms)][BF_4], where M = Mo (**12**), W (**13**). In this case, only η^2-propene exchange reaction takes place, and the moiety with η^5-indenyl and intramolecular coordination remains unchanged. On the other hand, reaction with CH_3CN leads to rapid $\eta^5 \rightarrow \eta^3$ haptotropic rearrangement of indenyl to afford [{η^3:κN-1-(C_9H_6N)C_9H_6}M(CO)$_2$($NCCH_3$)$_2$][BF_4], where M = Mo (**14**), W (**15**). In this case, the η^3-Ind coordination is surprisingly stable, with no tendency to reverse $\eta^3 \rightarrow \eta^5$ ring slippage, which was previously well described for the parent species with unsubstituted indenyl. To bring insight into this unusually stable low-coordination mode of the π-ligand, a series of quantum-chemical calculation were performed. In the first instance, the system [(η^3-Ind)Mo($NCCH_3$)$_3$(CO)$_2$]$^+$ ↔ [(η^5-Ind)Mo($NCCH_3$)$_2$(CO)$_2$]$^+$ was theoretical studied in detail. The calculated energy profile of this haptotropic rearrangement revealed that the position of indenyl ligand toward [M(CO)$_2$] fragment considerably affects the activation energy of the ring slippage. This means that the rotation of the indenyl ligand is a key step of haptotropic rearrangement. In the case of compounds **14** and **15**, the intramolecular coordination blocks the rotation meaning stabilization of η^3-coordination of the π-ligand.

List of references

[1] B. M. Trost, M. C. Ryan, *Angew. Chemie Int. Ed.* **2017**, *56*, 2862–2879.
[2] J. Ascenso, I. S. Gonçalves, E. Herdtweck, C. C. Romão, *J. Organomet. Chem.* **1996**, *508*, 169–181.
[3] C. A. Gamelas, N. A. G. Bandeira, C. C. L. Pereira, M. J. Calhorda, E. Herdtweck, M. Machuqueiro, C. C. Romao, L. F. Veiros, *Dalt. Trans.* **2011**, *40*, 10513–10525.
[4] J. Honzíček, J. Vinklárek, M. Erben, J. Lodinský, L. Dostál, Z. Padělková, *Organometallics* **2013**, *32*, 3502–3511.
[5] J. Honzíček, I. Honzíčková, J. Vinklárek, Z. Růžičková, *J. Organomet. Chem.* **2014**, *772–773*, 299–306.
[6] J. Lodinsky, J. Vinklarek, L. Dostal, Z. Ruzickova, J. Honzicek, *RSC Adv.* **2015**, *5*, 27140–27153.
[7] M. Enders, P. Fernández, G. Ludwig, H. Pritzkow, *Organometallics* **2001**, *20*, 5005–5007.
[8] M. L. Buil, M. A. Esteruelas, A. M. López, A. C. Mateo, E. Oñate, *Organometallics* **2007**, *26*, 554–565.
[9] I. S. Gonçalves, C. C. Romão, *J. Organomet. Chem.* **1995**, *486*, 155–161.
[10] J. R. Ascenso, C. G. de Azevedo, I. S. Goncalves, E. Herdtweck, D. S. Moreno, C. C. Romao, J. Zuehlke, *Organometallics* **1994**, *13*, 429–431.
[11] J. R. Ascenso, C. G. de Azevedo, I. S. Goncalves, E. Herdtweck, D. S. Moreno, M. Pessanha, C. C. Romao, *Organometallics* **1995**, *14*, 3901–3919.
[12] M. J. Frisch, G. W. Trucks, H. B. Schlegel, G. E. Scuseria, M. A. Robb, J. R. Cheeseman, G. Scalmani, V. Barone, B. Mennucci, G. A. Petersson, et al., *Gaussian 09, Revis. B.01, Gaussian, Inc., Wallingford CT* **2009**.
[13] A. D. Becke, *Phys. Rev. A* **1988**, *38*, 3098–3100.
[14] A. D. Becke, *J. Chem. Phys.* **1993**, *98*, 5648–5652.
[15] C. Lee, W. Yang, R. G. Parr, *Phys. Rev. B* **1988**, *37*, 785–789.
[16] B. Miehlich, A. Savin, H. Stoll, H. Preuss, *Chem. Phys. Lett.* **1989**, *157*, 200–206.
[17] K. A. Peterson, D. Figgen, M. Dolg, H. Stoll, *J. Chem. Phys.* **2007**, *126*, 124101.
[18] C. Peng, H. Bernhard Schlegel, *Isr. J. Chem.* **1993**, *33*, 449–454.
[19] C. Peng, P. Y. Ayala, H. B. Schlegel, M. J. Frisch, *J. Comput. Chem.* **1996**, *17*, 49–56.
[20] J. Tomasi, B. Mennucci, R. Cammi, *Chem. Rev.* **2005**, *105*, 2999–3094.
[21] J. Hou, Z. Tan, Y. Yan, Y. He, C. Yang, Y. Li, *J. Am. Chem. Soc.* **2006**, *128*, 4911–4916.
[22] M. Enders, P. Fernández, M. Kaschke, G. Kohl, G. Ludwig, H. Pritzkow, R. Rudolph, *J. Organomet. Chem.* **2002**, *641*, 81–89.
[23] M. Bottrill, M. Green, *J. Chem. Soc. Dalt. Trans.* **1977**, 2365–2371.
[24] J. Honzíček, J. Vinklárek, Z. Padělková, L. Šebestová, K. Foltánová, M. Řezáčová, *J. Organomet. Chem.* **2012**, *716*, 258–268.
[25] O. Mrózek, J. Vinklárek, Z. Růžičková, J. Honzíček, *Eur. J. Inorg. Chem.* **2016**, *2016*, 5250–5264.
[26] J. W. Faller, C.-C. Chen, M. J. Mattina, A. Jakubowski, *J. Organomet. Chem.* **1973**, *52*, 361–386.
[27] O. Mrózek, L. Šebestová, J. Vinklárek, M. Řezáčová, A. Eisner, Z. Růžičková, J. Honzíček, *Eur. J. Inorg. Chem.* **2016**, *2016*, 519–529.

[28] J. Markham, K. Menard, A. Cutler, *Inorg. Chem.* **1985**, *24*, 1581–1587.
[29] G. R. Fulmer, A. J. M. Miller, N. H. Sherden, H. E. Gottlieb, A. Nudelman, B. M. Stoltz, J. E. Bercaw, K. I. Goldberg, *Organometallics* **2010**, *29*, 2176–2179.
[30] J. Vinklárek, H. Hurychová, J. Honzíček, L. Šebestová, Z. Padělková, M. Řezáčová, *Eur. J. Inorg. Chem.* **2013**, *2013*, 2665–2672.
[31] K. Strohfeldt, M. Tacke, *Chem. Soc. Rev.* **2008**, *37*, 1174–1187.
[32] C. A. Gamelas, E. Herdtweck, J. P. Lopes, C. C. Romão, *Organometallics* **1999**, *18*, 506–515.
[33] L. S. Bartell, E. A. Roth, C. D. Hollowell, K. Kuchitsu, J. E. Young, *J. Chem. Phys.* **1965**, *42*, 2683–2686.
[34] L. J. Guggenberger, P. Meakin, F. N. Tebbe, *J. Am. Chem. Soc.* **1974**, *96*, 5420–5427.
[35] M. V Joannou, M. J. Bezdek, K. Al-Bahily, I. Korobkov, P. J. Chirik, *Organometallics* **2017**, *36*, 4215–4223.
[36] J. Pinkas, I. Císařová, R. Gyepes, J. Kubišta, M. Horáček, K. Mach, *Organometallics* **2012**, *31*, 5478–5493.
[37] O. Mrózek, J. Vinklárek, L. Dostál, Z. Růžičková, J. Honzíček, *Polyhedron* **2018**, *150*, 35–39.
[38] N. Cabon, F. Y. Pétillon, P. Schollhammer, J. Talarmin, K. W. Muir, *J. Organomet. Chem.* **2006**, *691*, 566–572.
[39] N. Kuhn, E. Zauder, R. Boese, D. Bläser, *J. Chem. Soc. Dalt. Trans.* **1988**, 2171–2175.
[40] M. A. Fard, A. Behnia, R. J. Puddephatt, *Organometallics* **2018**, *37*, 3368–3377.
[41] Y.-P. Chang, A. L. Hector, W. Levason, G. Reid, J. Whittam, *Dalt. Trans.* **2018**, *47*, 2406–2414.
[42] E. L. Muetterties, *J. Am. Chem. Soc.* **1969**, *91*, 1636–1643.
[43] E. L. Muetterties, *J. Am. Chem. Soc.* **1969**, *91*, 4115–4122.
[44] R. Asatryan, E. Ruckenstein, J. Hachmann, *Chem. Sci.* **2017**, *8*, 5512–5525.

List of Published Works

Papers in impacted international journals in the topic of the thesis:

1) Indenyl Compounds with Constrained Hapticity: The Effect of Strong Intramolecular Coordination, O. Mrózek, J. Vinklárek, Z. Růžičková, and J. Honzíček, *Eur. J. Inorg. Chem*. **2016**, 5250–5264.

2) Enhanced cytotoxicity of indenyl molybdenum(II) compounds bearing a thiophene function, O. Mrózek, L. Melounková, L. Dostál, I. Císařová, A. Eisner, R. Havelek, E. Peterová, J. Honzíček and J. Vinklárek, *Dalton Trans*., **2019**, 48, 11361−11373.

3) Propene complexes of molybdenum and tungsten stabilized by intramolecular coordination of 1-(quinol-8-yl)indenyl ligand, O. Mrózek, L. Dostál, I. Císařová, J. Honzíček and J. Vinklárek, *Dalton Trans*., **2019**, in press.

Papers in impacted international journals out of the topic of the thesis:

1) Highly Water-Soluble Cyclopentadienyl and Indenyl Molybdenum(II) Complexes - Second Generation of Molybdenum-Based Cytotoxic Agents, O. Mrózek, L. Šebestová, J. Vinklárek, M. Řezáčová, A. Eisner, Z. Růžičková, and J. Honzíček, *Eur. J. Inorg. Chem*. **2016**, 519–529.

2) Stabilization of two coordinate tetrylene by borylamide ligand, M. Aman, O. Mrózek, L. Dostál, Z. Růžičková, R. Jambor, *J. of Organomet. Chem.* **2018**, 872, 1–7.

3) Sorption of Sr(II) onto nanocomposites of graphene oxide-polymeric matrix, M. Bubeníková, P. Ecorchard, L. Szatmáry, O. Mrózek, P. Salačová, J. Tolasz, *Journal of Radioanalytical and Nuclear Chemistry* **2018**, 315, 263–272.

4) Molybdenum complexes of poly[(methylthio)methyl]borates, O. Mrózek, J. Vinklárek, L. Dostál, Z. Růžičková, J. Honzíček, *Polyhedron* **2018**, 150, 35–39.

5) Mg-Al-La LDH-MnFe2O4 hybrid material for facile removal of anionic dyes from aqueous solutions, O. Mrózek, P. Ecorchard, P. Vomáčka, J. Ederer, D. Smržová, M. Šrámová Slušná, A. Machálková, M. Nevoralová, H. Beneš, *Applied Clay Science* **2018**, 169, 1–9.

List of Conference Contributions

Poster presentations:

1) O. Mrózek, J. Honzíček, I. Císařová, J. Vinklárek, Constrained-hapticity complexes: impact of strong intramolecular coordination, XXXIV GEQO Congress Organometallic Chemistry Group, Girona (Spain), **September 7–9, 2016**, Book of abstracts, page 199.
2) O. Mrózek, J. Vinklárek, J. Honzíček, New approach for stabilization of low-hapticity indenyl complexes, EuChemS International Organometallic Conference XXII, Amsterdam, The Netherlands – Beurs van Berlage, **July 9–13, 2016**, Book of abstracts, poster 156.
3) O. Mrózek, J. Vinklárek, J. Honzíček, I. Císařová, Indenyl Complexes of Molybdenum and Tungsten with Strong Intramolecular Coordination, XXVIII International Conference on Organometallic Chemistry, Florence, Italy, **July 15–20, 2018**, Book of abstracts, P100.

Oral presentations:

1) O. Mrózek, J. Honzíček and J. Vinklárek, Cyclopentadienyl molybdenum compounds with intramolecular coordination, 16th International Seminar of PhD Students on Organometallic and Coordination Chemistry, Schloss Schney, Lichtenfels, Germany, **October 17–21, 2015**, Book of Abstracts, P40.
2) O. Mrózek, J. Honzíček and J. Vinklárek, Kinetická stabilizace η^3-indenylových komplexů, 2. konference Pokroky anorganické chemie, Kutná Hora, **19.–21. 6. 2016**, Czech Chem. Soc. Symp. Ser. 14, 147 (2016), ISSN 2336-7210 (On-line).
3) O. Mrózek, J. Honzíček, I. Císařová, J. Vinklárek, The stabilization of low-hapticity complexes by intramolecular coordination, 17th International Seminar of PhD Students on Organometallic and Coordination Chemistry, Kraskov, Czech Republic, **April 2–6, 2017**, Program an Abstracts, OP21.
4) O. Mrózek, Jaromír Vinklárek, Jan Honzíček and Ivana Císařová, Propene complexes of molybdenum and tungsten, 23rd Conference on Organometallic Chemistry, Helsinki, Finland, **June 16–20**, 2019, Book of Abstracts O35.